Initial imperfections for fea of tubular beams based on validated experiment results

Pavlovic, Marko; Veljkovic, Milan

Publication date
2016

Document Version
Accepted author manuscript

Published in
The International Colloquium on Stability and Ductility of Steel Structures

INITIAL IMPERFECTIONS FOR FEA OF TUBULAR BEAMS BASED ON VALIDATED EXPERIMENT RESULTS

Marko Pavlović and Milan Veljković

Delft University of Technology, Faculty of Civil Engineering and Geosciences (CITG), Delft, The Netherlands

Abstract: The experiment data available on 4-point bending experiments performed in Australia and Europe on tubular section beams are validated by FEA. Large scattering of available experiment results is investigated by detailed analysis of different geometrical imperfections. Loading set-up is analysed through modelling of welding induced imperfections. It is found that the welding induced imperfections lead to more accurate prediction of the local buckling failure modes and the rotation capacity than the traditionally modelled geometrical Eigen-mode imperfections. Also the influence of measured residual stresses is examined.

1. Introduction

Resistance and rotation capacity of tubular beams depend on strength of the material but also the local buckling which is influenced by slenderness of the cross section and real imperfections: geometric, residual stresses and inhomogeneity of the material. Large scattering of experiment data on the resistance and rotation capacity is present in published experiment results, such as [1] for I beams, which is used as basis for current cross section classification rules in the Eurocode both for open and closed cross sections. Results of 4–point bending experiments on tubular beams [4], [5] and [8] also show large scattering, especially in terms of rotation capacity, see Fig. 1. Reasons for such large scattering are differences in set-ups: cross-section and beam scale and loading point detail, but also on initial imperfections which depend on production process and type of the material: cold-formed, hot-finished, mild steel, HS steel, etc. The most unfavourable equivalent wave-like shape geometric imperfections obtained in linear buckling Eigen-mode analysis are used in state-of-the-art buckling FEA to validate the experiment results and for parametric studies. However, measurements of imperfections on mild steel and high strength steel hollow section beams [4], [6], [8] and [9] report constant longitudinal distribution of mostly convex, “bow-out” geometric imperfection in a wide amplitude range, approximately 1/100 – 1/1000.

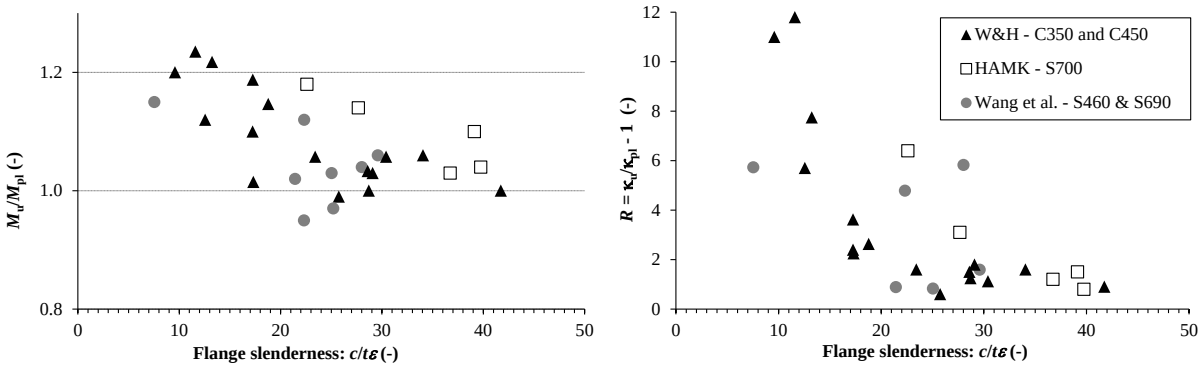

a) Non-dimensional bending resistance b) Rotation capacity

Fig. 1: Scattering experiment results from [4], [5] and [8]

a) Wilkinson and Hancock [4] b) HAMK experiments [5] c) Wang et al. [8]

Fig. 2: Local web and flange buckling near the loading point in bending experiments

Scattering of Eigen-mode imperfections amplitudes used to validate experiment results of different research is also large and do not coincide in shape, nor in amplitude with the measured imperfections [7], [8]. EN 1993-1-5 [2] recommends equivalent bow imperfection of the local subpanel in a cross section as 1/200, either as one bow or a wave-like shape imperfection.

Local buckling in 3-point and 4-point bending experiments occurs in the vicinity of the loading point, see Fig. 2. Wilkinson and Hancock [4] used loading detail by welding side plates over the full height of the web. In HAMK experiments side plates are welded only in the bottom half of the web in order to prevent welding imperfections in the compression zone of the hollow section. Wang et al. [8] applied force by direct contact over the thick plate.

Residual stresses dependent on the forming process (continuous forming, direct forming) might also affect the local buckling. Almost zero membrane residual stresses are obtained in several independent experimental research, see [13]. However, significant bending residual stresses, between 50% and 90% of the yield strength, are observed in the longitudinal and transverse direction of the tubular beam.

Welding imperfections are suspected to have major influence on local buckling in analysed experiments. Therefore they are validated by FEA where welding induced imperfections and residual stresses due to forming are applied. Afterwards, the influence of welding induced imperfections is compared to currently used equivalent geometric imperfections.

2. FE model of reference experiments

The finite element modelling (FEM) in ABAQUS finite element software package [3] is validated by 4-point bending experiments of hollow section beams: on shorter beams having spans between 1.3 and 1.7 m made of S460 performed by Wilkinson and Hancock [4] and on longer span beams made of S700 having spans from 3 m to 6.8 m performed by HAMK [5]. Cold-formed hollow sections are produced in continuous forming (CF) process in both cases.

Totally 9 cases are analysed having wide range of spans, cross-section dimensions, thicknesses and aspect ratios, see [14].

Experiments are modelled using shell elements S3D4r at the outer surface for the beam and solid elements C3D8R for loading plates and welds with proper coupling by tie constraint surface pairs, see Fig. 3. Two vertical plane symmetry boundary conditions is exploited in FEA. Loading point details differences between [4] and [5] experiments, in terms of height of the weld on the web, are carefully taken into account. Exact material properties obtained in coupon tensile tests of each specimen in bending experiments are considered in FEA. Different material properties are used for the flange and the web, according to coupon tests results. General/Static solver with load application by displacement is used in Abaqus [3].

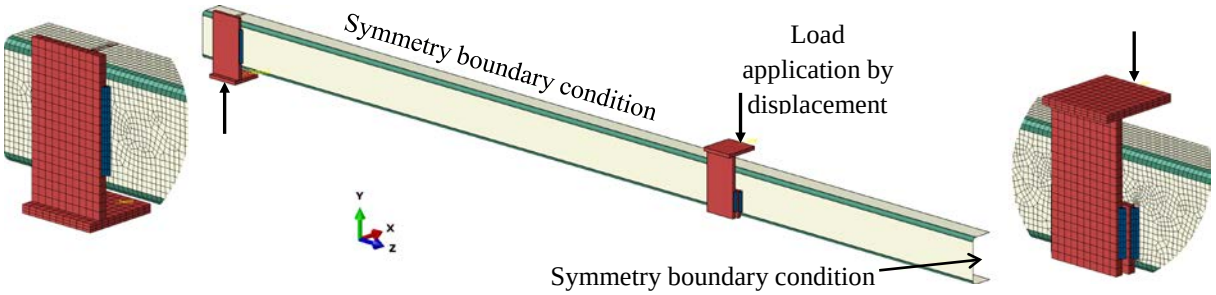

Fig. 3: FE model of 4-point bending experiments

3. Initial imperfections

3.1. Welding induced imperfections

Welding of steel plates causes local deformations and residual stresses in heat affected zone (HAZ). Angular distortion, also called the transverse bending (TB) [10], shown in Fig. 4a, is the most important in the case of side plates welded to the web of the hollow section beam analysed in this study because it produces the critical local geometrical imperfection. The amount of angular distortion due to welding depends on many parameters, such as: type of the weld and welding technique, input heat, thickness of the plates and the weld, etc. However, research results published in [10], [11], combining experiments and thermo-elastic-plastic (TEP) analysis of bead on plate and T-joint fillet welds showed that the angular distortion has an limiting value of $TB_{\text{lim}} = 0.022$ rad, depending mostly on the input heat and thickness of the plate see Fig. 4.

Prediction of welding induced deformations is employed by inherent strain method (ISM). Conservatively, the extreme angular distortion due to welding available in literature $TB = 0.022$ rad is used in FEA of 4-point bending as geometrical imperfection. TEP analysis is performed on plain strain 2D model of the longitudinal section in the middle of the height of the weld in Abaqus Welding Interface (AWI) [12], see Fig. 5. The aim was to obtain the model of distribution of the plastic strains in the HAZ and weld, producing the angular distortion. Effective width of longitudinal plastic strains in the web below the weld is estimated as given in Eq. (1), where a_w is the weld throat thickness. For the prescribed value of the angular distortion TB, see Fig. 5c, the induced strain ε_w at the outer face of the web is given in Eq. (2).

$$b_{w,\text{eff}} = 1.5 a_w \sqrt{2} \tag{1}$$

$$\varepsilon_w = TB \cdot t / b_{w,\text{eff}} \tag{2}$$

Based on the model of distribution the effective width $b_{w,\text{eff}}$ and the induced strain ε_w are calculated for each case considered in FE validation of 4-point experiments and applied to the

4-point bending FE model, see Fig. 6. Strains are applied only in longitudinal direction of the beam using orthotropic expansion properties of the material and distribution shown in Fig. 5b.

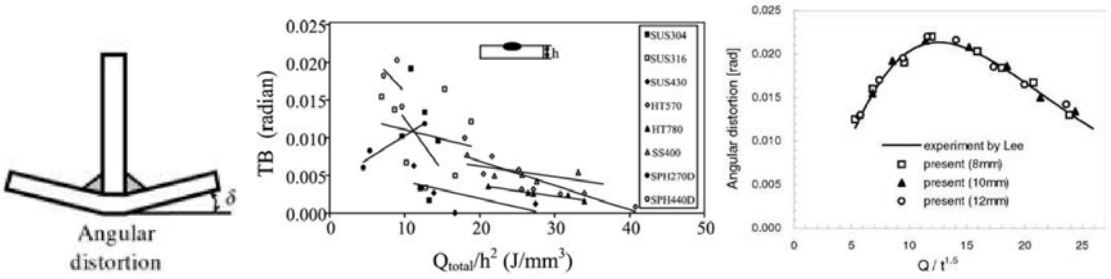

a Shape of distortion b) bead-on-plate welds, 3-5 mm [11] c) fillet welds, plates 8-10 mm [10]

Fig. 4: Transverse bending (angular distortion) due to welding

a) TEP analysis of fillet weld between the web and the loading plate

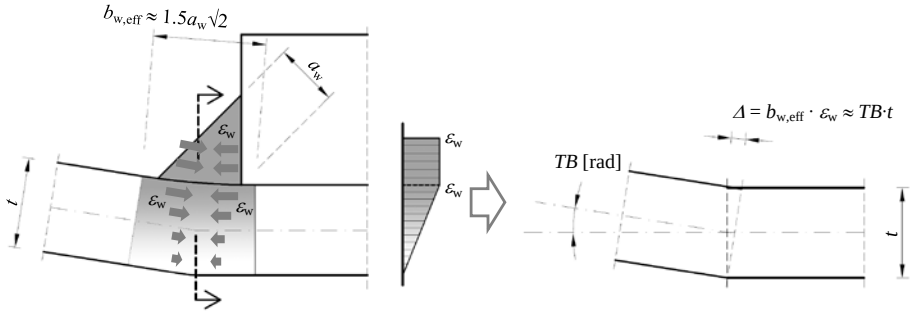

b) induced strain distribution c) induced strain vs. angular distortion *TB*

Fig. 5: Model of welding induced plastic strain distribution.

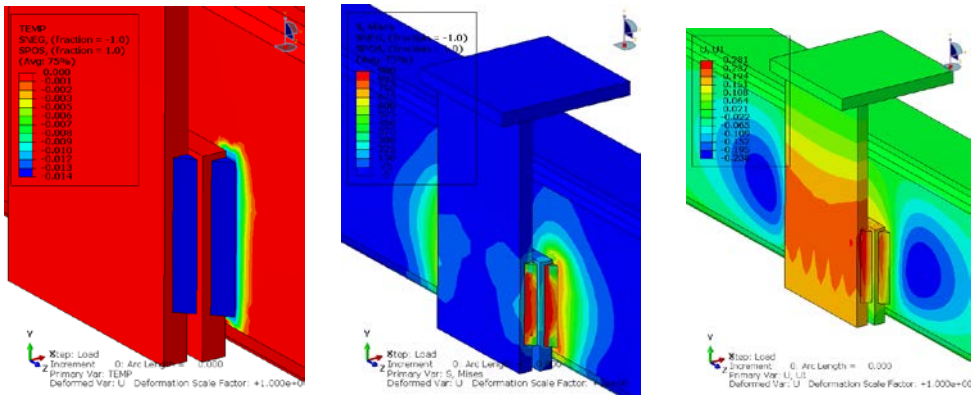

a) strains applied by temperature b) von Mises stresses c) out of plane deformations

Fig. 6: Welding induced strains applied in FE model of RHS 140×140×6

3.2. Residual stresses

Bending residual stresses are indirectly applied in FEA by equivalent temperature strains using orthotropic thermal expansion material properties to define different signs of the longitudinal and transverse direction, see [14]. Application of approximately 50 % of the yield strength residual stresses is achieved.

3.3. Equivalent geometric imperfections

Influence of geometric imperfections in form of Eigen-shape and bow-out imperfections, shown in Fig. 7, are analysed with the aim to show their influence on the scattering of rotation capacity obtained in experiments, in comparison to welding induced imperfections. Square hollow sections from the larger scale experiments [5] and nominal material properties of S500, S700 and S960 materials are used, see [14]. Two sets of imperfection amplitudes are analysed: a) 1/700 – comparable to the imperfections obtained by applying welding induced angular distortions and b) 1/200 – according to EN 1993-1-5 [2] recommendation.

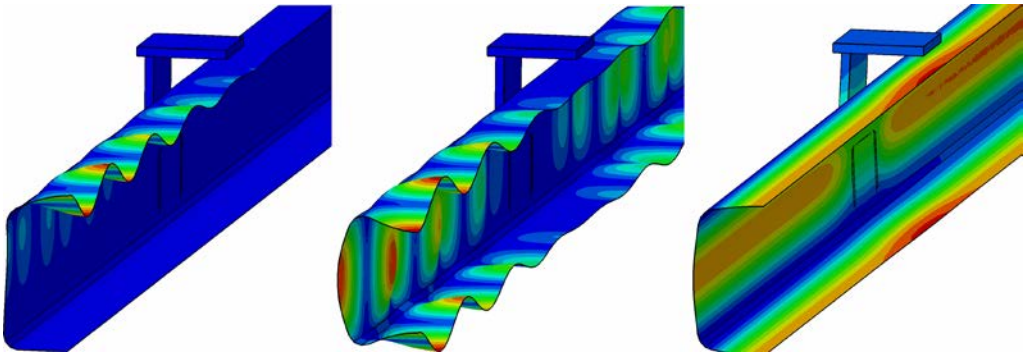

a) Eigen-mode due to bending load b) Eigen-mode due to axial load c) "bow-out" imperfections

Fig. 7: Typical equivalent geometric imperfections used in nonlinear analysis

4. Results and discussion

4.1. Welding induced imperfections vs. residual stresses

Influence of different imperfections are presented in Fig. 8 and Fig. 9: a) without any imperfections, b) with welding induced imperfections only, c) with residual stresses only and d) with welding induced imperfections and residual stresses. Ultimate resistance is well estimated by FEA even if no imperfections are applied. However, the rotation capacity is overestimated and in most of the cases the obtained failure mode in FEA does not reflect experiments because the local buckling occurs in the mid-span of the beam.

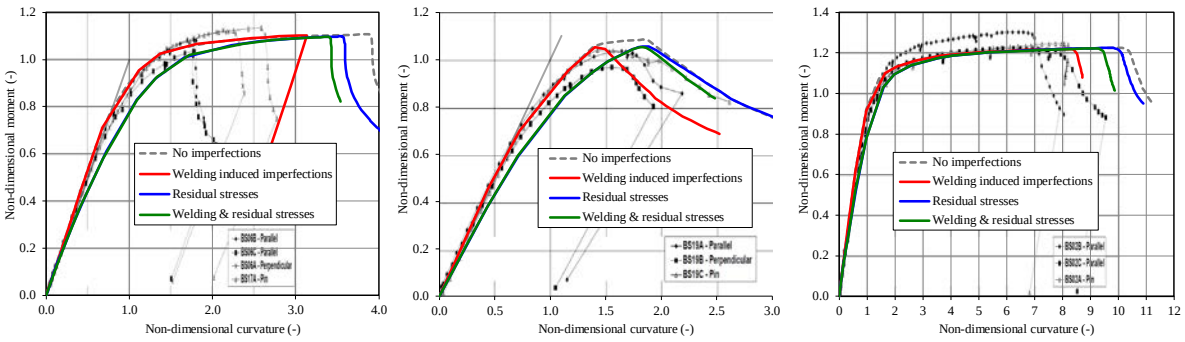

a) RHS 100x50x2 b) SHS 100x100x3 c) RHS 150x50x4

Fig. 8: Experiment [4] vs. FE results

Applying welding imperfections gives very good results in terms of prediction of rotation capacity, see Fig. 8 and Fig. 9. Also the characteristic failure mode obtained in experiments, local buckling near the loading plates, is obtained in each case in FEA, see Fig. 10. If only the residual stresses are applied as defined in section 0 the obtained rotation capacities are overestimated. The square hollow sections showed the same behaviour as if no imperfections are

applied and in case of the rectangular hollow sections only up to 10% reduction of the rotation capacity is obtained. If both the welding imperfections and residual stresses are applied the rotation capacity is increased compared to the case where only welding imperfections are applied. Finally, it is concluded that best agreement between the experiment and FEA results is obtained if only welding induced imperfections are applied in FEA of 4- point bending of hollow section beams.

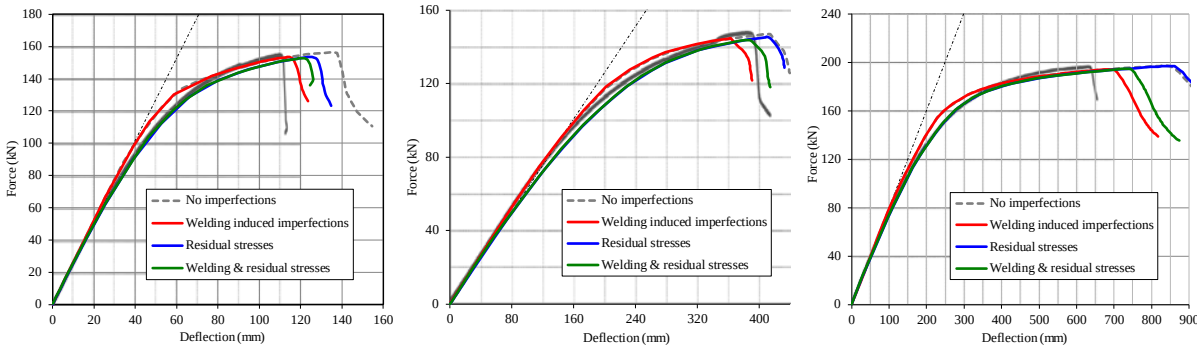

a) RHS 150x100x4 c) SHS 150x150x6 d) SHS 150x150x8

Fig. 9: Experiment [5] vs. FE results

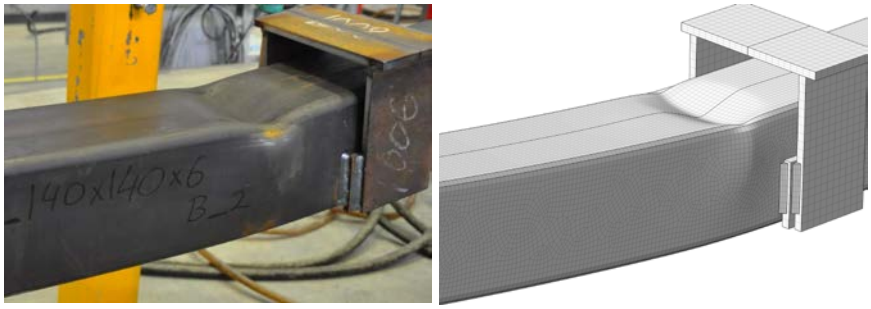

Fig. 10: Failure mode in experiments vs. FEA with welding induced imperfections

4.2. Welding induced imperfections vs. equivalent geometric imperfections

Large scattering of non-dimensional bending resistance and rotation capacity is obtained with the analysed imperfection parameters, see Fig. 11. The average variation ranges of the obtained results are 0.15 and 3 for the bending resistance and the rotation capacity, respectively. Similar scattering can be observed in experiments, see Fig. 1.

Higher resistance and capacity is obtained with bow-out imperfections having amplitude 1/200, compared to the welding induced imperfections having equivalent amplitude of 1/700. This leads to the conclusion that in absence of loading plates welded to the hollow section, higher ductility of the hollow section beams can be obtained.

Much lower bending resistance and rotation capacity is obtained with equivalent Eigen-mode imperfections, compared to the welding induced and bow-out imperfections. The influence of the Eigen-mode imperfection shape (caused either by bending or axial loads), is insignificant compared to influence of the imperfection amplitude. It is concluded that applying the Eigen-mode equivalent geometric imperfection with amplitude 1/200, according to EN 1995-1-5 [2], is unrealistic compared to behaviour obtained with more realistic welding induced imperfections.

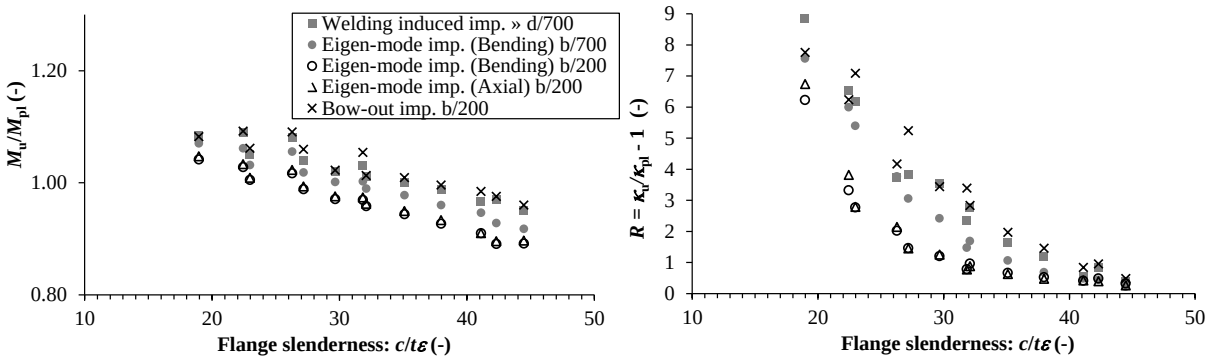

a) Non-dimensional bending resistance b) Rotation capacity

Fig. 11: FEA results for high-strength steel with different imperfections

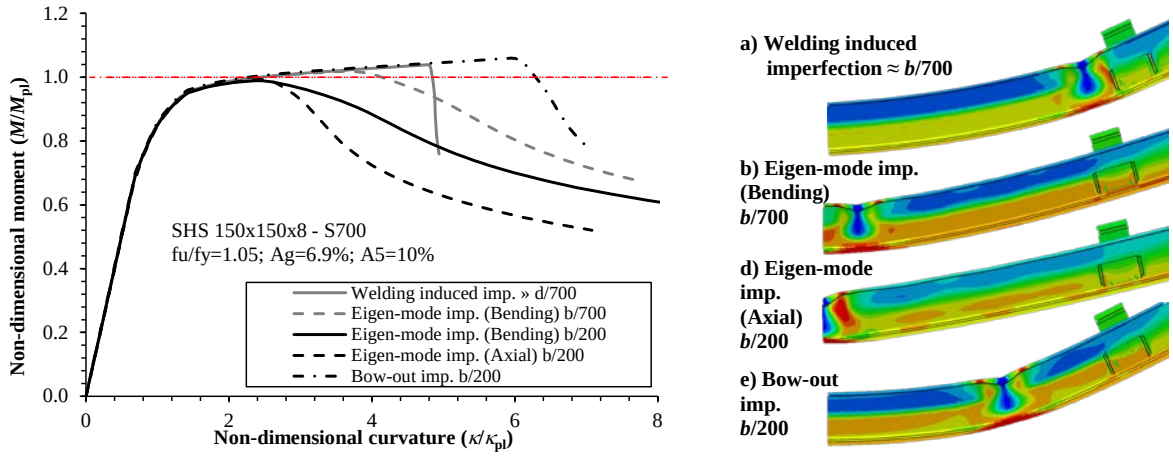

Fig. 12: Moment-rotation curves and location of local buckling with different imperfections

Influence of the imperfection type on post buckling behaviour is shown in Fig. 12 by non-dimensional moment-rotation curves and by location of the local buckling. The local buckling near the loading point in case of the welding induced and bow-out imperfections results in sudden reduction of the bending moment and therefore lower rotation capacity. This is related to the fact that the curvature is calculated based on differences of the deflections at the loading points and at the mid-span of the beam. Once the plastic hinge is formed at the loading point in case of the welding induced imperfections, the three points have constant increase of the deflections and the calculated curvature is almost constant. In case of the bow-out-imperfections the local buckling occurs a bit towards the mid-span and therefore the described phenomenon is less pronounced. In case of the Eigen-mode imperfections the local buckling in the mid span influence the increase of difference in deflections of the loading points and the mid-span and therefore the curvature rapidly increases.

It is concluded that the rotation capacity in the 4-point bending experiments is influenced by position of the local buckling between the loading points (the region of the constant bending moment) which is the additional reason for large scattering of experiment results.

5. Conclusions

Following conclusions are drawn from the study:

1. FEA validation of series of experiment results clearly showed the dominating influence of welding induced imperfections compared to the influence of residual stresses.

2. Least scattering of the experiment results is obtained in experiments where the loading plates are welded only to the part of the cross section which is in tension. This loading detail is recommended for the 4-point bending set-up.
3. The Eigen-mode equivalent geometric imperfection with amplitude 1/200, according to EN 1995-1-5 [3], leads to a bit pessimistic results compared to calculations using the welding induced imperfections.

Acknowledgments

This work was partially supported by RFCS through the Research Project RUOSTE. The authors gratefully acknowledge Prof. Markku Heinisuo for providing valuable information for the project.

References

[1] Sedlacek G, Feldmann M. "The b/t ratios controlling the applicability of analysis models in Eurocode 3, Part 1.1", *Background Document 5.09 for chapter 5 of Eurocode, Part 1.1*, Aachen, Germany 1995.

[2] EN-1993-1-5: *Design of steel structures, Part 1-5: Plated structural elements*, Brussels, Belgium, European Committee for Standardization, 2006.

[3] *ABAQUS Version 6.13 Analysis User's Guide*, 3DS Simulia, 2014.

[4] Wilkinson T, Hancock G. *Tests for the compact web slenderness of cold-formed rectangular hollow sections*, Research Report R744, The University of Sydney 1997.

[5] Zhongcheng M, Havula J. *Bending tests of S700 tubes*, Report 2015-56, University of Applied Sciences HAMK, Hämeenlinna, Finland 2015.

[6] *RUOSTE Project - Background Document on Deliverable 2.2 – Local buckling*. RFCS 2016.

[7] Wilkinson T, Hancock G. *Finite element analysis of plastic bending of cold-formed rectangular hollow section beams*, Research Report R792, The University of Sydney 1999.

[8] Wang J, Afshan S, Gkantou M, Theofanous M, Baniotopoulos C, Gardner L. "Flexural behaviour of hot-finnished high strength seet square and rectangular hollow sections", *Journal of Construction al Steel Research*, 121, 97-109, 2016.

[9] Ma JL, Chan TM, Young B. "Experimental Investigation on Stub-Column Behavior of Cold-Formed High-Strength Steel Tubular Sections", *Journal of Structural Engineering ASCE*, 2015.

[10] Jang CD, Lee CH, Ko DE. "Prediction of welding deformations of stiffened panels", *Proc. Instn. Mech. Engrs., Part M: J Engineering for the Maritime Enviroment*, Vol. 216, 133-143, 2002.

[11] Wang R, Zhang J, Serizawa H, Murakawa H. "Study of welding inherent deformations in thin plates based on finite element analysis using interactive substructure method", *Materials and Design*, 30, 3274-3481, 2009.

[12] *ABAQUS Extensions: Abaqus Welding Interface*, 3DS Simulia, 2015.

[13] *RUOSTE Project - Background Document on Deliverable 2.1 – Residual Stress Measurements*. RFCS 2016.

[14] *RUOSTE Project - Background Document on Deliverable 1.5 – Rotation capacity of beams*. RFCS 2016.